

3D-QSAR comparative molecular field analysis on delta opioid receptor agonist SNC80 and its analogs

Youyi Peng, Susan M. Keenan, Qiang Zhang, William J. Welsh*

Department of Pharmacology, University of Medicine & Dentistry of New Jersey-Robert Wood Johnson Medical School (UMDNJ-RWJMS), and the Informatics Institute of UMDNJ, Piscataway, NJ 08854, USA

Received 14 December 2004; received in revised form 18 March 2005; accepted 21 March 2005

Available online 13 June 2005

Abstract

Three-dimensional quantitative structure–activity relationship (3D-QSAR) models were constructed using comparative molecular field analysis (CoMFA) for a series of δ opioid receptor agonists: SNC80 analogs. Quantum chemical calculations on SNC80 show that protonation is preferred at the basic N4 atom over the alternative N1 atom, accordingly N4 protonation may contribute significantly to ligand–receptor interactions under physiologically relevant conditions. Statistically significant and predictive CoMFA models were achieved by pooling biological data from independent published sources, including compounds with both αR and αS benzylic configurations. Improved CoMFA models were obtained when the compounds were considered as N4-protonated species rather than neutral compounds. The influence of various atomic partial-charge formalisms, alignment schemes and additional molecular descriptors was evaluated in order to produce the highest quality models. In addition, separate CoMFA models were generated for compounds with only the αR benzylic configuration. These CoMFA models showed excellent internal predictability and consistency, and external validation using test-set compounds yielded predicted pIC_{50} values within 1 log unit of the corresponding experimentally measured values. Key insights into the structure–activity relationship derived from the CoMFA analysis concur with experimentally observed data, thus the CoMFA models presented here find utility for predicting the binding affinity, and guiding the design, of novel SNC80 analogs and related δ opioid receptor agonists.

© 2005 Elsevier Inc. All rights reserved.

Keywords: Opioid receptors; Agonists; SNC80; CoMFA; N4-protonated forms

1. Introduction

The existence of at least three distinct subtypes of opioid receptors in the central nervous system (CNS) and periphery is well established [1,2]. Opioid receptors belong to the superfamily of G-protein coupled receptors (GPCRs), and the three isoforms exhibit 60% amino acid sequence identity [3–5]. Studies have shown that each opioid receptor is differentially distributed in the CNS and periphery and mediates unique pharmacological responses [4,5]. Opioid receptor agonists are involved in the modulation of numerous pharmacological activities. Recent evidence has shown that δ -selective agonists show promise as analgesics devoid of the numerous side effects (such as respiratory depression and physical dependence) associated with morphine and other μ

receptor agonists [6]. In addition to their potential use as analgesics, δ receptor agonists have been reported to stimulate respiration [7], act as antidiarrheals [8,9] and antidepressants [10,11], and elicit immunomodulatory effects mediated through δ -like opioid receptors on the surface of immune cells [5,12,13]. More recently, δ opioid selective agonists (e.g., SNC80) have exhibited potent antiparkinsonian activity in both rat and primate models [14].

SNC80, (+)-4-[(αR)- α -(2*S*,5*R*)-4-allyl-2,5-dimethyl-1-piperazinyl]-3-methoxybenzyl]-*N,N*-diethylbenzamide, is a highly selective (selectivity ratio $\mu/\delta = 857$, $\kappa/\delta = 2438$ in rat brain membranes) and potent δ opioid receptor agonist ($IC_{50} = 2.9$ nM in rat brain membranes)[15]. SNC80 has attracted significant interest by virtue of its unique structure (Fig. 1) compared with the classical nonpeptidic opiates such as naltrindole (NTI, Fig. 1) [15–19]. The interaction between opioid receptors and their ligands has been described in terms of the familiar “message-address” concept [20,21], which

* Corresponding author. Tel.: +1 732 235 3234; fax: +1 732 235 3475.
E-mail address: welshwj@umdnj.edu (W.J. Welsh).

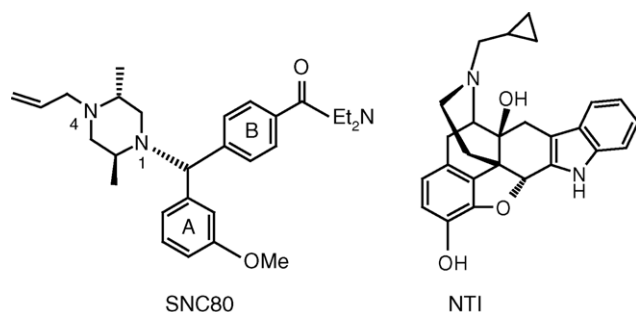


Fig. 1. Structures of (+)SNC80 (left) and NTI (right). Numbers indicate the atom positions in the systematic name of SNC80.

suggests that all opioid receptor active compounds share common pharmacophore patterns. The “message” represents those structural features common to all opioids that are recognized similarly by the three types of receptors (δ , κ and μ). The “address” represents those specific structural features that confer high selectivity for a particular (e.g., δ) opioid receptor. For NTI, a δ selective antagonist with a morphine-like structure, the tyramine moiety corresponds to the “message” while the conformationally constrained benzene ring linked to the morphinan nucleus acts as the “address”. In SNC80 (Fig. 1), the methoxyphenyl/N4 region may correspond to the “message” while the diethylamide is believed to be the nonaromatic “address” for the δ opioid receptor [22]. New δ agonists have been reported by incorporating this nonaromatic address into classical opiate structures [23].

Molecular modeling techniques are valuable tools for drug design and can be used to quantify and visualize interactions of ligands with their target receptors. Three-dimensional (3D) quantitative structure–activity relationship (3D-QSAR) models constructed by employing comparative molecular field analysis (CoMFA) are particularly effective in cases when the receptor structure is unknown. CoMFA samples the steric and electrostatic fields surrounding a set of ligands and constructs a 3D-QSAR model by correlating these 3D fields with the corresponding experimental activities. The primary aim of this study was to develop predictive 3D-QSAR models for a series of SNC80 analogs to rationalize the receptor–ligand interactions of δ opioid receptor agonists. These models should prove useful for the rational design of novel and potent δ opioid receptor agonists with numerous pharmacological applications such as powerful yet safe analgesics, immunomodulatory agents for treating immune disorders and antiparkinsonian agents. The utility of such 3D-QSAR models for opioid receptor active compounds is especially compelling in view of absence of X-ray crystallographic structural data for this pharmacologically important member of the G-protein coupled superfamily of receptors.

2. Methods

All molecular modeling operations were performed on Silicon Graphics, Inc. (SGI) workstations. The crystal

structure of (–)SNC80 was used as the starting conformation for building the molecular structures [24]. Experimental analysis suggests that the N4 atom, but not the N1 atom, of (+)SNC80 (Fig. 1) is crucial for tight binding to the δ opioid receptor [25]. Here, a computational approach was employed to further explore this observation. The energies of (+)SNC80 separately as N1- and N4-protonated species were calculated using three methods: the Tripos force field and both the AM1 and ab initio HF/6-31G** quantum mechanical methods accessed through Spartan’02 [26] to compare their relative stabilities (Table 1). Next, all compounds were built with Sybyl 6.8 molecular modeling software package [27] in both neutral and N4-protonated forms. The MMFF94 force field and default partial atomic charges were used to optimize the geometries of all compounds. In addition, Gasteiger–Hückel charges were calculated to evaluate the influence of various partial atomic-charge schemes on the resultant models. (+)SNC80 was selected as the template for aligning all the compounds in the training- and test-sets since it is highly active and the crystal structure of its epimer is known [24]. Two alignment rules were studied to examine the influence of different alignments: *atom fit* and *field fit*. Specifically, three atoms were chosen for atom fit: the basic nitrogen N4 and the two centroids of ring A and B (Fig. 1). The atom-fit alignment of all molecules protonated on the N4 atom is shown in Fig. 2. In *field fit*, the steric and electrostatic fields of all compounds were aligned to those of (+)SNC80. Two additional molecular descriptors, viz., the HOMO (E_{HOMO}) and LUMO (E_{LUMO}) molecular orbital energies, were calculated for N4-protonated forms using the AM1 method implemented in Spartan’02 [26] and incorporated into the CoMFA model development.

2.1. Biological data

Data from three separate articles published by the same research group (using identical binding assay protocols) were combined for the present CoMFA studies [15–17]. Briefly, competitive binding assays were performed against rat-brain membrane by using [^3H]-DADLE to label the δ receptor binding site. For the sake of consistency, K_i values for these compounds published by Furness et al. [16] were converted to

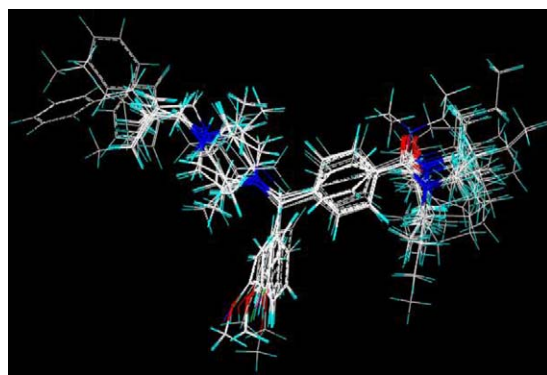


Fig. 2. Atom-fit alignment of N4-protonated SNC80 analogs in both αR and αS configurations. Molecules are colored by Sybyl atom-type.

IC₅₀s based on the familiar Cheng–Prusoff equation. The K_d value of [³H]-DADLE (1.7 nM) was kindly provided by Dr. Christina M. Dersch of the NIH-NIDDK. A total of 54 compounds with appreciable binding affinity for the δ receptor were pooled, yielding a data set that spanned >3 logarithmic (log) units in terms of pIC₅₀ and contained both αR and αS benzylic configurations (Table 2). Furthermore, the biological activity of the data set compounds is evenly distributed with 15 weakly active compounds (pIC₅₀ < 7.0), 20 moderately active compounds (7.0 < pIC₅₀ < 8.0), and 19 highly active compounds (pIC₅₀ > 8.0). The data set was divided into a training-set (45 compounds) to develop CoMFA models and a test-set (9 compounds) for model validation. The test-set compounds were chosen randomly with a slight bias toward ensuring representation from the full range of biological data and structural variations in the training-set. The resulting test-set contained three weakly active, three moderately active and three highly active compounds. The structures and binding affinities (pIC₅₀) of all compounds are shown in Table 2.

2.2. CoMFA procedure

(+)-SNC80 was selected as the template for aligning all the compounds in the training and test-sets since it is highly active and the crystal structure of its epimer is known [24]. The standard CoMFA procedure implemented in Sybyl 6.8 was performed. Each δ agonist was placed in a 3D grid lattice separated by 2 Å. A C_{sp3} atom with a formal charge of +1 and a van der Waals radius of 1.52 Å served as the probe. The steric (van der Waals) and electrostatic (Coulombic) interactions were calculated at each grid point by summing the individual interaction energies between each atom of the opioid agonist molecules and the probe atom. A distance dependent dielectric function $\epsilon = \epsilon_0 R_{ij}$ with $\epsilon_0 = 1.0$ was adopted to apply Coulomb's law. Maximum field values were truncated to 30 kcal/mol for the steric fields and to ± 30 kcal/mol for the electrostatic fields.

2.3. Partial least-square analysis

The partial least-square (PLS) technique was employed to generate a linear regression between changes in the steric and electrostatic fields and changes in binding affinity (pIC₅₀) of the training-set compounds. The CoMFA potential fields represent the independent variables, while pIC₅₀ represents

the dependent variable for PLS analysis which converts the steric and electrostatic fields to principal components (PCs) consisting of linear combinations of the original independent variables. To assess the internal predictive ability of the CoMFA models, we employed “leave-one data set-out” cross-validation together with the standard “leave-one-out” cross-validation. In this procedure, each data set or compound is excluded one at a time, after which its activity is predicted by the model constructed from the remaining compounds in the training-set. Cross-validation determines the optimum number of PCs, corresponding to the smallest error of prediction and the highest $r_{cv}^2(q^2)$. PLS analysis was repeated without validation using the optimum number of PCs to generate a final CoMFA model from which the conventional r^2 (a measure of the internal consistency of the model) and related statistical parameters were derived. These parameters include the F -ratio [28], defined as $r^2/(1-r^2)$, corresponding to the ratio of properties explained by the CoMFA model to those not explained by it. In order to improve efficiency and reduce “noise”, a column filter was employed to exclude these columns whose grid-point energies varied <2.0 kcal/mol. All CoMFA models are displayed in color contour maps which enable visualization of the 3D steric fields that significantly contribute to a model.

3. Results and discussion

3.1. Energy calculations for protonated SNC80

The piperazine ring of (+)-SNC80 contains two nitrogen atoms N1 and N4 (Fig. 1). The N4 atom is crucial for SNC80's potent binding affinity to the δ opioid receptor since replacement of this N atom by an O atom or C atom abolishes δ binding affinity [25]. In contrast, replacement of the N1 atom by a C atom reveals only a marginal effect on δ binding affinity. In order to explore this observation computationally, values of the energy of (+)-SNC80 protonated separately at N1 and N4 were calculated assuming both gas-phase and aqueous-solvated conditions by three separate approaches, viz., molecular mechanics using the Tripos force field, and quantum mechanics at both the AM1 and HF/6-31G** levels of theory as implemented in Spartan'02 [26]. The SM5.4 implicit solvation model accessed in Spartan was employed to simulate aqueous conditions. In all cases considered here, the results show that protonation of (+)-SNC80 is energetically

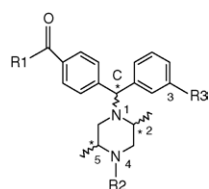
Table 1
Calculated values of the energy (kcal/mol) of SNC80 protonated at N1 or N4 atom

	Tripos force field		AM1		HF/6-31G**	
	Vacuum	Aqueous	Vacuum	Aqueous	Vacuum	Aqueous
E_{N1}	33.50	−7.74	145.24	104.57	−876275.00	−876315.00
E_{N4}	30.44	−18.09	144.86	99.43	−876277.00	−876323.00
ΔE	3.06	10.35	0.38	5.14	2.00	8.00

E_{N1} : Energy of protonated SNC80 at N1 atom; E_{N4} : energy of protonated SNC80 at N4 atom; $\Delta E = E_{N1} - E_{N4}$.

Table 2

Structures and binding affinity of all compounds in the pooled data set




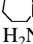

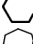
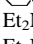
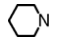
No.	C α	C ₂	C ₅	R1	R2	R3	pIC ₅₀		Residual	Ref.
							Experimental	Predicted		
(+)SNC80	R	S	R	Et ₂ N	Allyl	OMe	8.49	8.28	0.21	[16]
1	R	S	R	Et ₂ N	H	OMe	7.99	8.06	−0.07	[16]
2	R	S	R	Et ₂ N	Methyl	OMe	8.01	8.06	−0.05	[16]
4	R	S	R	Et ₂ N	<i>n</i> -Butyl	OMe	8.23	7.88	0.35	[16]
5	R	S	R	Et ₂ N	<i>n</i> -Pentyl	OMe	7.99	7.75	0.24	[16]
6	R	S	R	Et ₂ N	<i>n</i> -Hexyl	OMe	7.65	7.71	−0.06	[16]
7	R	S	R	Et ₂ N	2-MeAllyl	OMe	7.98	7.99	−0.01	[16]
8	R	S	R	Et ₂ N	Crotyl	OMe	8.38	8.24	0.14	[16]
10	R	S	R	Et ₂ N	Benzyl	OMe	7.87	7.92	−0.05	[16]
11	R	S	R	Et ₂ N	2-PhEthyl	OMe	7.18	7.56	−0.38	[16]
12	R	S	R	Et ₂ N	3-PhPropyl	OMe	7.44	7.69	−0.25	[16]
13	R	S	R	Et ₂ N	Allyl	OH	8.82	9.03	−0.21	[15]
14	S	R	S	Et ₂ N	Allyl	OH	7.23	6.79	0.44	[15]
15	S	R	S	Et ₂ N	Allyl	OMe	6.37	6.29	0.08	[15]
16	R	S	R	Et ₂ N	Allyl	H	9.02	8.72	0.30	[15]
18	R	S	R	Et ₂ N	Allyl	F	8.53	8.70	−0.17	[15]
19	S	R	S	Et ₂ N	Allyl	F	5.86	6.47	−0.61	[15]
20	R	S	R	Et ₂ N	Allyl	I	8.41	8.53	−0.12	[15]
21	R	R	S	Et ₂ N	Allyl	OMe	8.31	7.93	0.38	[15]
22	S	S	R	Et ₂ N	Allyl	OMe	7.20	7.08	0.12	[15]
23	R	R	S	Et ₂ N	Allyl	H	8.04	8.15	−0.11	[15]
25	R	R	S	Et ₂ N	Allyl	F	8.32	8.17	0.15	[15]
26	S	S	R	Et ₂ N	Allyl	F	7.20	7.37	−0.17	[15]
27	S	S	R	Et ₂ N	Allyl	I	7.39	7.37	0.02	[15]
29	S	S	R	Et ₂ N	Allyl	OH	7.94	7.72	0.22	[15]
30	R	S	R	H ₂ N	Allyl	OMe	6.35	6.07	0.28	[17]
31	R	S	R	EtNH	Allyl	OMe	6.82	6.80	0.02	[17]
32	R	S	R	Et ₂ CHNH	Allyl	OMe	6.75	6.84	−0.09	[17]
33	R	S	R	<i>t</i> -BuNH	Allyl	OMe	6.55	6.90	−0.35	[17]
35	R	S	R	Et(Me)N	Allyl	OMe	8.38	7.62	0.76	[17]
36	R	S	R	<i>n</i> -Pr ₂ N	Allyl	OMe	7.88	7.87	0.01	[17]
37	R	S	R	<i>i</i> -Pr ₂ N	Allyl	OMe	8.15	8.15	0.00	[17]
38	R	S	R	Et(<i>n</i> -Bu ₂)N	Allyl	OMe	8.18	8.14	0.04	[17]
39	R	S	R	<i>n</i> -Bu ₂ N	Allyl	OMe	7.46	7.98	−0.52	[17]
40	R	S	R		Allyl	OMe	7.74	7.78	−0.04	[17]
42	R	S	R		Allyl	OMe	8.09	8.06	0.03	[17]
43	S	S	R	H ₂ N	Allyl	OMe	6.41	6.33	0.08	[17]
44	S	S	R	EtNH	Allyl	OMe	7.46	7.40	0.06	[17]
45	S	S	R	Me ₂ N	Allyl	OMe	6.63	6.55	0.08	[17]
46	S	S	R	Et(Me)N	Allyl	OMe	7.22	6.69	0.53	[17]
47	S	S	R	<i>n</i> -Pr ₂ N	Allyl	OMe	6.82	6.83	−0.01	[17]
50	S	S	R	<i>n</i> -Bu ₂ N	Allyl	OMe	6.89	6.99	−0.10	[17]
51	S	S	R		Allyl	OMe	6.58	7.24	−0.66	[17]
52	S	S	R		Allyl	OMe	6.35	6.64	−0.29	[17]
53	S	S	R		Allyl	OMe	6.91	6.90	0.01	[17]
3*	R	S	R	Et ₂ N	Ethyl	OMe	7.95	8.02	−0.07	[16]
9*	R	S	R	Et ₂ N	CPM	OMe	8.12	7.97	0.15	[16]
17*	S	R	S	Et ₂ N	Allyl	H	6.07	6.65	−0.58	[15]
24*	S	S	R	Et ₂ N	Allyl	H	7.22	7.52	−0.30	[15]
28*	R	R	S	Et ₂ N	Allyl	OH	8.76	7.96	0.80	[15]
34*	R	S	R	Me ₂ N	Allyl	OMe	8.32	7.71	0.61	[17]

Table 2 (Continued)

No.	C α	C ₂	C ₅	R1	R2	R3	pIC ₅₀		Residual	Ref.
							Experimental	Predicted		
41*	R	S	R		Allyl	OMe	7.84	7.78	0.06	[17]
48*	S	S	R	i-Pr ₂ N	Allyl	OMe	6.46	7.01	−0.55	[17]
49*	S	S	R	Et(<i>n</i> -Bu ₂)N	Allyl	OMe	6.82	6.98	−0.16	[17]

Compounds in the test-set are denoted by a star (*).

preferred at N4 over N1 (Table 1). These calculations suggest that (+)SNC80 binds to the δ opioid receptor as an N4-protonated species and that the basicity (and, indeed, the presence) of the N1 atom is not a critical factor, in accordance with experimental findings. Based on these results, protonation of (+)SNC80 and its analogs was considered exclusively at the N4 atom in the present study.

3.2. CoMFA model development for compounds with α R and α S configurations

In order to achieve a statistically significant 3D-QSAR model, certain criteria to select the original data set must be satisfied. Usually, the biological activity of targeted ligands should be evenly distributed and span ≥ 3 log units. Furthermore, the compounds employed to build the model should number ≥ 20 . Since both intra- and inter-laboratory variations in pharmacological data are virtually unavoidable, all possible efforts should be taken to obtain the biological data from a single source. When this is not possible, as is the case with SNC80 analogs, extra precautions should be taken to validate mixing of multi-source data. In view of the important clinical implications of SNC80 and other agonists selective for the δ opioid receptor, we decided to pool biological data from separate articles to amass a sufficient number of compounds for 3D-QSAR model development. One mandatory requirement for pooling data is that the biological data be derived using identical experimental protocols. We retrieved biological data from three independent publications, each of which reported results for SNC80 analogs using the same assay [15–17]. Separately, each data set does not fulfill the necessary requirements for model development. Collectively however, the combined data set of 54 ligands (Table 2) exhibits biological activity which is evenly distributed across >3 log units of δ binding affinity (pIC₅₀).

In order to examine the feasibility of utilizing the pooled data, preliminary CoMFA models were constructed with all compounds in their N4-protonated forms. A process of “leave-one data set-out”, similar to “leave-one-out” cross-validation implemented in standard PLS analysis, was carried out in which ligands from each single source (i.e., set S1 listed in Table 3) were systematically excluded from the training data set and served as the test-set for model validation. Standard PLS analysis was performed for the remaining compounds (Model S1). The statistics associated with the CoMFA models using MMFF94 charges are shown in Table 3. Each CoMFA model (Models S1–S3) produced

Table 3

Statistical parameters obtained from preliminary CoMFA models

	PC	q^2	SEE ^a	r^2	F
Model total ^b	3	0.74	0.29	0.87	111
Model S1 [16]	3	0.74	0.33	0.86	82
Model S2 [15]	3	0.68	0.26	0.87	76
Model S3 [17]	3	0.78	0.25	0.91	86

^a Standard error of estimate.

^b Including all molecules from the pooled data set.

strong indicators of statistical significance ($r^2 > 0.85$) and internal predictive ability ($q^2 > 0.60$) using only three PCs (Table 3). Predictions for the test-set compounds agreed with experiment with a residual <1 log unit. Our previous studies have shown that it is possible to build statistically robust and predictive CoMFA models by pooling biological data in this way [29].

Following the preliminary model development described above, the 54 compounds were divided into two subsets: training-set (45 compounds) and test-set (9 compounds). CoMFA-PLS studies were performed on the neutral (Model 1) and N4-protonated (Model 2) training-set compounds with MMFF94 atomic partial charges using an atom-fit alignment scheme. Both models showed good internal predictability and goodness of fit (Table 4), with the statistical quality (q^2) slightly better for the compounds as N4-protonated species than as neutral molecules. As these compounds would likely exist predominately in their protonated form under physiological conditions (pH 7.4), the N4-protonated species were selected for further studies. In order to evaluate the influence of different charge formalisms, separate models were constructed using Gasteiger–Hückel partial atomic charges with atom-fit alignment. The statistical significance and predictive ability of the models remained nearly constant ($q^2 = 0.63/r^2 \cong 0.85$), indicating that these CoMFA models are essentially invariant to different choices of charge

Table 4

Statistical parameters obtained from the final CoMFA models

Model no.	Models ^a	No. of PCs	q^2	r^2	SEE	F
1	N, MMFF94, atom	3	0.58	0.85	0.31	75
2	P, MMFF94, atom	3	0.63	0.85	0.31	78
3	P, MMFF94, field	3	0.55	0.87	0.29	90
4	Model 2 + E_{HOMO}	4	0.61	0.86	0.33	63
5	Model 2 + E_{LUMO}	4	0.59	0.86	0.31	59
6	P, MMFF94, atom	4	0.60	0.94	0.16	97

^a N: neutral; P: N4-protonated; atom: atom-fit alignment; field: field-fit alignment; E_{HOMO} : HOMO molecular orbital energy; E_{LUMO} : LUMO molecular orbital energy.

formalisms. A separate model (Model 3 in Table 4) was constructed in which molecular alignment was performed using field-fit instead of atom-fit. Field-fit alignment allows molecules to adopt a common alignment by adjusting their geometries to minimize differences in their steric and electrostatic fields. Model 2 (MMFF charges, atom fit) yielded the best statistical performance and, therefore, was selected for further studies.

Standard CoMFA procedures implemented in Sybyl 6.8 take into account both steric and electrostatic fields. The influence of different physicochemical properties was explored by adding E_{HOMO} and E_{LUMO} to the standard CoMFA fields of Model 2. Molecular orbital energies have been reported as useful descriptors when the ligand–receptor interactions involves ionic or charge transfer [30,31]. However, the addition of molecular orbital energies into the CoMFA fields failed to improve the statistical results in our studies (Models 4 and 5 in Table 4). This situation may result from: (1) the protonated ligands used to derive the CoMFA models in the present studies already consider the fact that the ligands act as proton acceptors during ligand–receptor interaction or (2) the ligand–receptor interactions are dominated by the steric fields (~70%) over electrostatic fields (~30%). Indeed, a previous CoMFA model [29] based on a series of NTI analogs was dominated by steric effects. Here, our studies indicate that the descriptors extracted from steric and electrostatic fields are sufficient to explain the ligand binding affinity for the δ opioid receptor. The experimental and CoMFA-predicted (by Model 2) pIC_{50} s of the training-set compounds are listed in Table 2 and plotted in Fig. 3.

The predictive power of CoMFA Model 2 was validated using the test-set. Test-set compounds were selected quasi-randomly with a bias imposed to ensure structural variation and uniform coverage of biological activity. Comparison of the experimentally observed and CoMFA-predicted pIC_{50} values of test-set compounds (Table 2 and Fig. 3) further confirms the predictive ability of the model. The residuals (differences) between corresponding values of the experimental and predicted binding affinity are <1 log unit, and all test-set compounds follow the regression trend line established by the training-set.

3.3. CoMFA model development for compounds with αR configurations

Studies reported by Calderon and co-workers [32] reveal that the benzylic (α position in Table 2) configuration of SNC80 analogs is the most important stereochemical determinant of δ receptor binding affinity and selectivity. Therefore initially compounds with both αR and αS benzylic configurations were included in the pooled data set. We next attempted to develop separate CoMFA models for αR and αS compounds to differentiate the structural preferences for ligand binding. The αS compounds exhibit much lower δ binding affinity compared with the corresponding αR compounds to the extent that CoMFA model development

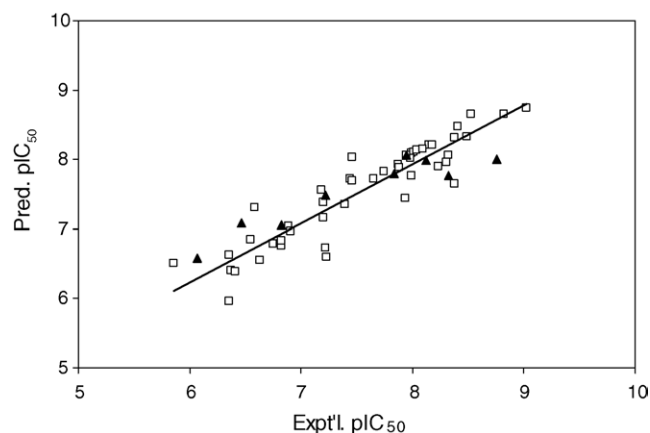


Fig. 3. Plot of CoMFA-predicted vs. experimental pIC_{50} values of the training-set and test-set compounds in both αR and αS configurations. (□) Training-set compounds; (▲) test-set compounds.

is not warranted, therefore we constructed a CoMFA model exclusively for the αR compounds again employing MMFF94 atomic charges and an atom-fit alignment scheme

Table 5

Experimental and CoMFA-predicted pIC_{50} values of αR compounds

No.	pIC_{50}		Residual
	Experimental	Predicted	
(+)SNC80	8.49	8.67	−0.18
1	7.99	7.94	0.05
2	8.01	7.93	0.08
4	8.23	8.36	−0.13
5	7.99	8.12	−0.13
6	7.65	7.50	0.15
7	7.98	7.91	0.07
8	8.38	8.42	−0.04
9	8.12	8.05	0.07
10	7.87	7.86	0.01
11	7.18	7.06	0.12
13	8.82	8.94	−0.12
16	9.02	9.21	−0.19
18	8.53	8.30	0.23
20	8.41	8.23	0.18
21	8.31	8.54	−0.23
23	8.04	7.87	0.17
25	8.32	8.24	0.08
30	6.35	6.33	0.02
31	6.82	6.76	0.06
33	6.55	6.50	0.05
35	8.38	8.86	−0.48
36	7.88	7.83	0.05
37	8.15	7.96	0.19
38	8.18	8.53	−0.35
39	7.46	7.57	−0.11
40	7.74	7.55	0.19
41	7.84	7.64	0.20
42	8.09	8.11	−0.02
3 ^a	7.95	8.09	−0.14
12 ^a	7.44	8.06	−0.62
28 ^a	8.76	8.23	0.53
32 ^a	6.75	6.74	0.01
34 ^a	8.32	7.87	0.45

^a Compounds in the test-set.

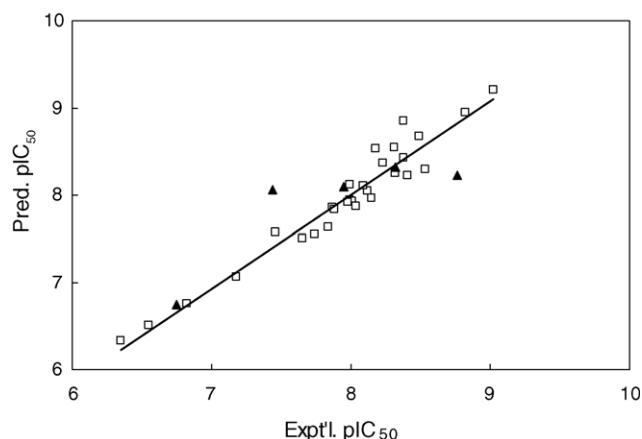


Fig. 4. Plot of CoMFA-predicted vs. experimental pIC_{50} values of the training-set and test-set compounds in the αR configuration only. (□) Training-set; (▲) test-set.

(Model 6 in Table 4). This model showed good internal predictability and self-consistency ($q^2 = 0.60/r^2 = 0.94$). The predictive ability of this model was validated using test-set compounds. The comparison of experimental and CoMFA-predicted pIC_{50} values of five test-set compounds reveals residuals of <1 log unit and good fit to the regression trend line (Table 5; Fig. 4).

3.4. Interpretation of the CoMFA models

CoMFA color-contour maps can be regarded as visual representations of the 3D-QSAR models. The colored polyhedra represent spatial regions around the ligands where variations in steric or electrostatic fields are associated with differences in the target property (i.e., pIC_{50}). The green (yellow) contours correspond to regions where increased steric bulk is favored (disfavored); the blue (red) contours correspond to regions where increased electropositive (electronegative) character is associated with enhanced ligand binding affinity. The CoMFA contour maps for Model

6 are shown in Fig. 5 with SNC80 and compound #33 inserted for visual clarity.

Close inspection of the CoMFA contour maps reveals that substitutions bulkier than allyl at N4 are not well tolerated for ligand binding to the δ opioid receptor. This observation, reflected by the yellow polyhedra appearing in the distal regions around N4, is consistent with the findings reported by Wei et al. [33] and Plobeck et al. [25], who discovered that increasing the size of N4 substituents on SNC80 analogs reduces the binding affinities at the δ opioid receptor. Yellow and blue polyhedra are found around position 3 of SNC80 (see Table 1 for SNC80 numbering), reflecting that bulky and electronegative substitutions (i.e., methoxy) at this position are unfavorable for enhancing δ binding affinity. No color polyhedron is located near position 2 and 5 of SNC80 (Table 1), which suggests that the two chiral centers are not necessary for high binding affinities at the δ opioid receptor. This result concurs with Plobeck et al. [25] who found that the compounds without the two methyl groups at positions 2 and 5 (i.e., *N,N*-diethyl-4-[phenyl(1-piperazinyl)methyl]-benzamide) retain strong δ binding affinity. The influence of steric and electrostatic substituent effects in the vicinity of the amide group are difficult to interpret. Subtle changes in the conformation of substituted amide group greatly influence the δ binding affinity, which concurs with the “address” role played by this group within the “message-address” concept. To assist visualization of substituent effects on the amide group, the monoalkylated compounds #33 and SNC80 are inserted into the electrostatic and steric maps. The comparison of contour maps with #33 (right) and SNC80 (left) superimposed for clarity indicates that disubstitutions are important for increasing ligand binding affinity since the substituent directed to the green polyhedra is structurally absent in compound #33. Increasing the steric bulk of the disubstituent at the amide group (i.e., *n*-butyl in compound #39) tends to lower δ binding affinity. The contour maps reflect differences in the orientation of the amide carbonyls of SNC80 and compound #33. Close examination of the alignment of all compounds with αR

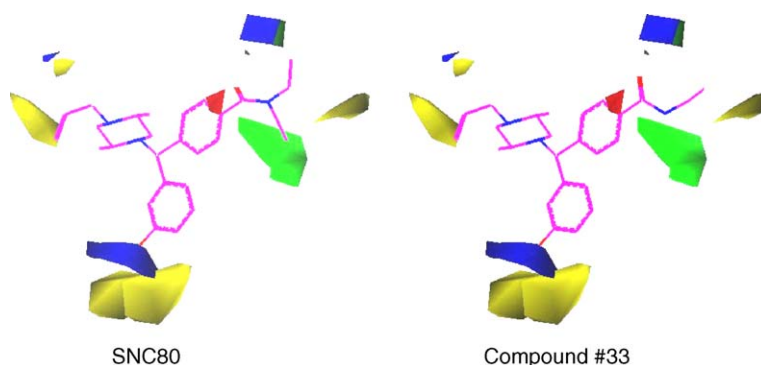


Fig. 5. CoMFA steric and electrostatic contour maps for δ opioid agonists. To assist visual clarity, SNC80 (left) and compound #33 (right) are inserted as ball-and-stick renderings with color-coded atom types: C (purple), N (blue) and O (red). Regions around the ligands where sterically bulky groups are favorable (unfavorable) for enhanced binding affinity are colored in green (yellow) accordingly. Similarly, regions where electronegative (red) and electropositive (blue) groups are favorable for enhanced ligand binding are colored accordingly.

configurations shows that monosubstituted (#31–33) and unsubstituted (#30) compounds have much smaller torsion angles between the phenyl plane and amide bond plane than disubstituted compounds (#34–42 and SNC80). The carbonyl at the amide group of SNC80 has been reported to form hydrogen bonding with the side chain of residue W284 at the third extracellular loop of the δ receptor [34,35]. The carbonyl should be aligned out of the plane of the phenyl ring in order to retain efficient binding to the δ opioid receptor [25]. After AM1 geometry optimization, the torsion angles were respectively 89° and 88° for SNC80 and #36 but 25° and 37° for #30 and #31. It is possible that the orientation of the amide carbonyl in monosubstituted and unsubstituted compounds impairs the capacity for hydrogen bonding and, thus, contributes to the sharp decrease in binding affinity (i.e., $IC_{50} = 451$ nM for #30, compared with $IC_{50} = 2.9$ nM for SNC80). This interpretation is consistent with the observations of Katsura et al. [17].

4. Conclusions

A 3D-QSAR study was performed in order to obtain insight into the structure–activity relationship of δ opioid receptor agonists: SNC80 analogs. Energy calculations confirm that protonation is preferred at N4 over N1 in SNC80, consequently N4 protonation likely plays an important role in stabilizing ligand–receptor interactions. Statistically significant CoMFA models were derived based on a pooled data set from independent sources including both αR and αS benzylic configurations. CoMFA models with atom-fit alignment exhibited better statistical parameters assuming the molecules as N4-protonated rather than neutral species. The CoMFA model derived from MMFF94 charges and atom-fit alignment exhibited excellent internal predictive ability and self-consistency. The influence of different atomic partial charge formalisms and alignment schemes on CoMFA models were also evaluated and found to be negligible. Likewise, inclusion of HOMO and LUMO molecular orbital energies along with the standard CoMFA fields had a negligible effect on the CoMFA model. A separate CoMFA model was developed for compounds with only αR benzylic configuration. These CoMFA models showed excellent internal predictability and consistency, and external validation using test-set compounds yielded a predicted pIC_{50} value within 1 log unit of the experimental value.

Inspection of the steric and electrostatic contour maps of CoMFA model for compounds in the αR configuration revealed that substituents more bulky than allyl at N4 of SNC80 are not well tolerated for δ binding affinity. Likewise, sterically bulky and electronegative substitutions at position 3 are unfavorable for enhanced binding affinity at δ opioid receptor. The CoMFA contour maps, together with the conformational alignment, indicate that disubstitution at the amide group is a crucial feature in dictating δ binding

affinity. It is hoped that these insights gained from the CoMFA models will be useful for the rational design of novel opioid receptor active agents and for prediction of their binding affinity at the δ opioid receptor.

Acknowledgments

Support for this research was provided by the Biotechnology Research & Development Corporation (BRDC, Peoria, IL), by a High-Technology Workforce Excellence Grant from the New Jersey Commission on High Education, and by the Informatics Institute of the University of Medicine and Dentistry of New Jersey.

References

- [1] B.N. Dhawan, F. Cesselin, R. Raghubir, T. Reisine, P.B. Bradley, P.S. Portoghesi, M. Hamon, International Union of Pharmacology. XII. Classification of opioid receptors, *Pharmacol. Rev.* 48 (1996) 567–592.
- [2] C.B. Pert, S.H. Snyder, Opiate receptor: demonstration in nervous tissue, *Science* 179 (1973) 1011–1014.
- [3] Y. Chen, A. Mestek, J. Liu, L. Yu, Molecular cloning of a rat kappa opioid receptor reveals sequence similarities to the mu and delta opioid receptors, *Biochem. J.* 295 (3) (1993) 625–628.
- [4] A. Goldstein, A. Naidu, Multiple opioid receptors: ligand selectivity profiles and binding site signatures, *Mol. Pharmacol.* 36 (1989) 265–272.
- [5] G.B. Stefano, P. Melchiorri, L. Negri, T.K. Hughes Jr., B. Scharrer, [D-Ala2]deltorphin I binding and pharmacological evidence for a special subtype of delta opioid receptor on human and invertebrate immune cells, *Proc. Natl. Acad. Sci. U.S.A.* 89 (1992) 9316–9320.
- [6] E.J. Bilsky, S.N. Calderon, T. Wang, R.N. Bernstein, P. Davis, V.J. Hruby, R.W. McNutt, R.B. Rothman, K.C. Rice, F. Porreca, SNC 80, a selective, nonpeptidic and systemically active opioid delta agonist, *J. Pharmacol. Exp. Ther.* 273 (1995) 359–366.
- [7] P.Y. Cheng, D. Wu, J. Decena, Y. Soong, S. McCabe, H.H. Szeto, Opioid-induced stimulation of fetal respiratory activity by [D-Ala2]-deltorphin I, *Eur. J. Pharmacol.* 230 (1993) 85–88.
- [8] M. Broccardo, G. Improta, Antidiarrheal and colonic antipropulsive effects of spinal and supraspinal administration of the natural delta opioid receptor agonist, [D-Ala2]deltorphin II, in the rat, *Eur. J. Pharmacol.* 218 (1992) 69–73.
- [9] M. Broccardo, G. Improta, A. Tabacco, Central effect of SNC 80, a selective and systemically active delta-opioid receptor agonist, on gastrointestinal propulsion in the mouse, *Eur. J. Pharmacol.* 342 (1998) 247–251.
- [10] P. Tejedor-Real, J.A. Mico, C. Smadja, R. Maldonado, B.P. Roques, J. Gilbert-Rahola, Involvement of delta-opioid receptors in the effects induced by endogenous enkephalins on learned helplessness model, *Eur. J. Pharmacol.* 354 (1998) 1–7.
- [11] A. Saitoh, Y. Kimura, T. Suzuki, K. Kawai, H. Nagase, J. Kamei, Potential anxiolytic and antidepressant-like activities of SNC80, a selective delta-opioid agonist, in behavioral models in rodents, *J. Pharmacol. Sci.* 95 (2004) 374–380.
- [12] D.J. Carr, C.H. Kim, B. deCosta, A.E. Jacobson, K.C. Rice, J.E. Blalock, Evidence for a delta-class opioid receptor on cells of the immune system, *Cell Immunol.* 116 (1988) 44–51.
- [13] D.J. Carr, B.R. DeCosta, C.H. Kim, A.E. Jacobson, V. Guarcello, K.C. Rice, J.E. Blalock, Opioid receptors on cells of the immune system:

- evidence for delta- and kappa-classes, *J. Endocrinol.* 122 (1989) 161–168.
- [14] C.J. Hille, S.H. Fox, Y.P. Maneuf, A.R. Crossman, J.M. Brotchie, Antiparkinsonian action of a delta opioid agonist in rodent and primate models of Parkinson's disease, *Exp. Neurol.* 172 (2001) 189–198.
- [15] S.N. Calderon, K.C. Rice, R.B. Rothman, F. Porreca, J.L. Flippen-Anderson, H. Kayakiri, H. Xu, K. Becketts, L.E. Smith, E.J. Bilsky, P. Davis, R. Horvath, Probes for narcotic receptor mediated phenomena. 23. Synthesis, opioid receptor binding, and bioassay of the highly selective delta agonist (+)-4-[(alphaR)-alpha-((2S,5R)-4-Allyl-2,5-dimethyl-1-piperazinyl)-3-methoxybenzyl]-N,N-diethylbenzamide (SNC80) and related novel nonpeptide delta opioid receptor ligands, *J. Med. Chem.* 40 (1997) 695–704.
- [16] M.S. Furness, X. Zhang, A. Coop, A.E. Jacobson, R.B. Rothman, C.M. Dersch, H. Xu, F. Porreca, K.C. Rice, Probes for narcotic receptor-mediated phenomena. 27. Synthesis and pharmacological evaluation of selective delta-opioid receptor agonists from 4-[(alphaR)-alpha-(2S,5R)-4-substituted-2,5-dimethyl-1-piperazinyl-3-methoxybenzyl]-N,N-diethylbenzamides and their enantiomers, *J. Med. Chem.* 43 (2000) 3193–3196.
- [17] Y. Katsura, X. Zhang, K. Homma, K.C. Rice, S.N. Calderon, R.B. Rothman, H.I. Yamamura, P. Davis, J.L. Flippen-Anderson, H. Xu, K. Becketts, E.J. Foltz, F. Porreca, Probes for narcotic receptor-mediated phenomena. 25. Synthesis and evaluation of N-alkyl-substituted (alpha-piperazinylbenzyl)benzamides as novel, highly selective delta opioid receptor agonists, *J. Med. Chem.* 40 (1997) 2936–2947.
- [18] J. Alfaro-Lopez, T. Okayama, K. Hosohata, P. Davis, F. Porreca, H.I. Yamamura, V.J. Hruby, Exploring the structure–activity relationships of inverted question mark 1-(4-tert-butyl-3'-hydroxy)benzhydryl-4-benzylpiperazine (SL-3111), a high-affinity and selective delta-opioid receptor nonpeptide agonist ligand, *J. Med. Chem.* 42 (1999) 5359–5368.
- [19] J.B. Thomas, X.M. Herault, R.B. Rothman, R.N. Atkinson, J.P. Burgess, S.W. Mascarella, C.M. Dersch, H. Xu, J.L. Flippen-Anderson, C.F. George, F.I. Carroll, Factors influencing agonist potency and selectivity for the opioid delta receptor are revealed in structure–activity relationship studies of the 4-[(N-substituted-4-piperidinyl)aryl-amino]-N,N-diethylbenzamides, *J. Med. Chem.* 44 (2001) 972–987.
- [20] R. Schwyzler, ACTH: a short introductory review, *Ann. N. Y. Acad. Sci.* 297 (1977) 3–26.
- [21] P.S. Portoghese, Bivalent ligands and the message-address concept in the design of selective opioid receptor antagonists, *Trends Pharmacol. Sci.* 10 (1989) 230–235.
- [22] S.H. Snyder, G.W. Pasternak, Historical review: opioid receptors, *Trends Pharmacol. Sci.* 24 (2003) 198–205.
- [23] G. Dondio, S. Ronzoni, D.S. Eggleston, M. Artico, P. Petrillo, G. Petrone, L. Visentin, C. Farina, V. Vecchiotti, G.D. Clarke, Discovery of a novel class of substituted pyrrolooctahydroisoquinolines as potent and selective delta opioid agonists, based on an extension of the message-address concept, *J. Med. Chem.* 40 (1997) 3192–3198.
- [24] F.H. Allen, The Cambridge Structural Database: a quarter of a million crystal structures and rising, *Acta Crystallogr. B* 58 (2002) 380–388.
- [25] N. Plobeck, D. Delorme, Z.Y. Wei, H. Yang, F. Zhou, P. Schwarz, L. Gawell, H. Gagnon, B. Pelcman, R. Schmidt, S.Y. Yue, C. Walpole, W. Brown, E. Zhou, M. Labarre, K. Payza, S. St-Onge, A. Kamassah, P.E. Morin, D. Projean, J. Ducharme, E. Roberts, New diarylmethylpiperazines as potent and selective nonpeptidic delta opioid receptor agonists with increased in vitro metabolic stability, *J. Med. Chem.* 43 (2000) 3878–3894.
- [26] Spartan'02, Wavefunction, Inc., Irvine, CA.
- [27] Sybyl 6.8, Tripos, Inc., St. Louis, MO.
- [28] D.L. Harnett, J.L. Murphy, Introductory Statistical Analysis, Addison-Wesley Publishing Co., Philippines, 1975, p. 430.
- [29] Y. Peng, S.M. Keenan, Q. Zhang, V. Kholodovych, W.J. Welsh, 3D-QSAR comparative molecular field analysis on opioid receptor antagonists: pooling data from different studies, *J. Med. Chem.* 48 (2005) 1620–1629.
- [30] S. Funar-Timofei, G. Schuurmann, Comparative molecular field analysis (CoMFA) of anionic azo dye-fiber affinities. I. Gas-phase molecular orbital descriptors, *J. Chem. Inf. Comput. Sci.* 42 (2002) 788–795.
- [31] C.L. Waller, G.R. Marshall, Three-dimensional quantitative structure–activity relationship of angiotensin-converting enzyme and thermolysin inhibitors. II. A comparison of CoMFA models incorporating molecular orbital fields and desolvation free energies based on active-analog and complementary-receptor-field alignment rules, *J. Med. Chem.* 36 (1993) 2390–2403.
- [32] S.N. Calderon, R.B. Rothman, F. Porreca, J.L. Flippen-Anderson, R.W. McNutt, H. Xu, L.E. Smith, E.J. Bilsky, P. Davis, K.C. Rice, Probes for narcotic receptor mediated phenomena. 19. Synthesis of (+)-4-[(alphaR)-alpha-((2S,5R)-4-allyl-2,5-dimethyl-1-piperazinyl)-3-methoxybenzyl]-N,N-diethylbenzamide (SNC 80): a highly selective, nonpeptide delta opioid receptor agonist, *J. Med. Chem.* 37 (1994) 2125–2128.
- [33] Z.Y. Wei, W. Brown, B. Takasaki, N. Plobeck, D. Delorme, F. Zhou, H. Yang, P. Jones, L. Gawell, H. Gagnon, R. Schmidt, S.Y. Yue, C. Walpole, K. Payza, S. St-Onge, M. Labarre, C. Godbout, A. Jakob, J. Butterworth, A. Kamassah, P.E. Morin, D. Projean, J. Ducharme, E. Roberts, N,N-Diethyl-4-(phenylpiperidin-4-ylidenemethyl)benzamide: a novel, exceptionally selective, potent delta opioid receptor agonist with oral bioavailability and its analogues, *J. Med. Chem.* 43 (2000) 3895–3905.
- [34] M. Valiquette, H.K. Vu, S.Y. Yue, C. Wahlestedt, P. Walker, Involvement of Trp-284, Val-296, and Val-297 of the human delta-opioid receptor in binding of delta-selective ligands, *J. Biol. Chem.* 271 (1996) 18789–18796.
- [35] M.C. Pepin, S.Y. Yue, E. Roberts, C. Wahlestedt, P. Walker, Novel “restoration of function” mutagenesis strategy to identify amino acids of the delta-opioid receptor involved in ligand binding, *J. Biol. Chem.* 272 (1997) 9260–9267.